Available online at www.sciencedirect.com
SCIENCE DIRECT®
Journal of Organometallic Chemistry 680 (2003) 312–322
Journal of Organometallic Chemistry
www.elsevier.com/locate/jorganchem

# Macropolyhedral boron-containing cluster chemistry. Aspects of the $S_2B_{16}H_{16}$ system. Preparation, structure, NMR spectroscopy and isomerism☆

Pervinder K. Dosangh [a,1], Jonathan Bould [a], Michael G.S. Londesborough [a,b], Tomáš Jelínek [a,b], Mark Thornton-Pett [a], Bohumil Štíbr [b], John D. Kennedy [a,*]

[a] The School of Chemistry of the University of Leeds, Leeds UK LS2 9JT, Northern England, EU, UK
[b] The Institute of Inorganic Chemistry of the Academy of Sciences of the Czech Republic, 25068 Řež-by-Prague, Czech Republic

Received 25 April 2003; received in revised form 17 May 2003; accepted 19 May 2003

It is a pleasure to be able to dedicate this paper to Prof. Fred Hawthorne in recognition of his sustained, formidable and incisive intellectual and experimental contributions over many many years to the field of boron-containing cluster chemistry

**Abstract**

Thermolysis of [*arachno*-4-$SB_8H_{12}$] (**1**) in boiling cyclohexane gives two isomers **2** and **3** of 18-vertex [$S_2B_{16}H_{16}$], together with known 12-vertex [*closo*-1-$SB_{11}H_{11}$] (**4**) and known 11-vertex [*nido*-7-$SB_{10}H_{12}$] (**5**). Compounds **2** and **3** are characterised by single-crystal X-ray diffraction analyses and single- and double-resonance $^{11}$B- and $^{1}$H-NMR spectroscopy. The [*n*-$S_2B_{16}H_{16}$] isomer **2** takes the form of *nido* ten-vertex: *nido* ten-vertex [*anti*-$B_{18}H_{22}$] with the 9 and 9′ positions occupied by S vertices, whereas the [*iso*-$S_2B_{16}H_{16}$] isomer **3** takes the form of a *nido* 11-vertex {$SB_{10}$} subcluster fused via a common two-boron edge to a *nido*-type {$B_8$} subcluster that is additionally linked *exo* to the {$SB_{10}$} subcluster by a bridging S atom that is held *endo* to the {$B_8$} unit. Isomer **2** is readily deprotonated and its monoanion **6** is characterised by NMR spectroscopy and by a single-crystal X-ray diffraction analysis of its [tmndH]$^+$[*n*-$S_2B_{16}H_{15}$] salt **6b**; deprotonation has occurred from an open-face B–H–B bridging site.


*Keywords:* Heteroborane cluster isomerism; Marcopolyhedral thiaborane; X-ray structures; Borane cluster compound; NMR spectroscopy

## 1. Introduction

Classically, polyhedral boron-containing cluster chemistry has a natural limit of cluster size at about the twelve-vertex icosahedron [1–3]. Although expansions of single clusters beyond the icosahedron to give species with thirteen or fourteen vertices are interestingly feasible [4–8], and although interesting big-molecule chemistry can result if boron-containing clusters are joined by sigma linkages or by metal atoms held in common [9–14], an extensive development of a contiguous borane cluster chemistry beyond the icosahedron requires the more intimate fusion of two or more clusters [15–17]. Of such fusions, the nine-vertex *arachno* system seems to favour thermal autofusions to generate such 'macropolyhedral' fused-cluster compounds, with [$B_9H_{13}(SMe_2)$] or [$B_9H_{13}(OBu_2)$] giving [*anti*-$B_{18}H_{22}$] [18,19], [$SB_8H_{10}(SMe_2)$] giving [$S_2B_{17}H_{17}(SMe_2)$] [20], and [$(CO)(PMe_3)_2HIrB_8H_{12}$] giving [$(CO)_2(PMe_3)_4Ir_2B_{16}H_{14}$] [21]; [$(PMe_2Ph)_2PtB_8H_{12}$] gives a variety of macropolyhedral platinaboranes, of

☆ This article was freely submitted for publication without royalty. By acceptance of this paper, the publisher and/or recipient acknowledges the right of the authors to retain non-exclusive, royalty-free license in and to any copyright covering this paper, along with the right to reproduce all or part of the copyrighted paper.

* Corresponding author. Tel.: +44-113-343-6414; fax: +44-113-343-6401.
*E-mail address:* johnk@chem.leeds.ac.uk (J.D. Kennedy).

[1] Formerly Pervinder Kaur, see Refs. [20,50]

0022-328X/03/$ - see front matter © 2003 Elsevier B.V. All rights reserved.
doi:10.1016/S0022-328X(03)00467-4

which $[(PMe_2Ph)_2Pt_2B_{12}H_{18}]$, $[(PMe_2Ph)_3Pt_2B_{16}H_{20}(PMe_2Ph)]$, $[(PMe_2Ph)PtB_{16}H_{18}(PMe_2Ph)]$, $[(PMe_2Ph)_4Pt_3B_{14}H_{16}]$, and $[(PMe_2Ph)_2Pt_2B_{16}H_{15}(C_6H_4Me)(PMe_2Ph)]$ have so far been identified [22–24]; $[(PPh_3)_2PdB_8H_{12}]$ gives $[(PPh_3)_4ClPd_4B_{16}H_{17}(PPh_3)]$ and $[(PMe_2Ph)_2PdB_8H_{12}]$ gives $[(PMe_2Ph)_2Pd_2B_{16}H_{22}(PMe_2Ph)_2]$ [24,25]. Here we now report results from the thermal autofusion of [*arachno*-4-$SB_8H_{12}$] (compound **1**, schematic cluster geometry **I**) to give two isomers of formulation $[S_2B_{16}H_{16}]$, which we designate [*n*-$S_2B_{16}H_{16}$] (**2**) and [*iso*-$S_2B_{16}H_{16}$] (**3**), each characterised by NMR spectroscopy and single-crystal X-ray diffraction analysis. Compounds **2** and **3** have quite different macropolyhedral structural architectures (schematic cluster geometries **II** and **III**, respectively). The NMR identification of the [*n*-$S_2B_{16}H_{16}$] isomer (compound **2**) has been reported in a preliminary communication [26], and additional preliminary and related aspects of the work have been presented at conferences [15,27–31]. Here we report more complete details. Note that in the schematic structural diagrams in this paper, unlabelled plain vertices correspond to {BH(*exo*)} units, and solid circles correspond to boron atoms with no *exo* substituents.

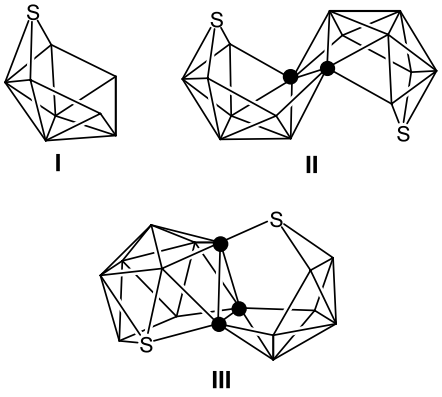


## 2. Results and discussion

The heating of [*arachno*-4-$SB_8H_{12}$] (compound **1**; schematic cluster geometry **I**) at reflux temperature in cyclohexane solution results in a few minutes in a mixture of two pale yellow eighteen-vertex isomers **2** and **3** of formulation $[S_2B_{16}H_{16}]$ (schematic skeletal geometries **II** and **III**, respectively), together with the known *closo* twelve-vertex cluster compound $[SB_{11}H_{11}]$ [32] (compound **4**; schematic cluster geometry **IV**) and a residue that is insoluble in common organic solvents and is presumed to consist of thiaborane polymers. No $[SB_8H_{12}]$ (**1**) remains. If the rapid generation of a sample mixture of compounds **2**, **3** and **4** is required, it is convenient to use the (dried) cyclohexane extract of crude $[SB_8H_{12}]$ that results from the oxidation of the [*nido*-6-$SB_9H_{11}]^-$ anion with acidic formaldehyde [33], without intermediate purification of the crude $[SB_8H_{12}]$. However, the recoverable yields of compounds **2** and **3** are then somewhat reduced, often considerably so. Yields, and relative proportions of products **2**, **3** and **4**, are in any event variable, and we have not so far been able to obtain consistent reproducibility over many preparations. Typical molar proportions of compounds **2**, **3** and **4**, as estimated by integrated NMR spectroscopy on product mixtures, are of the order of 4–18, 2–14 and 0–3%, respectively, although a 48% isolated yield of **2** was obtained in one experiment. Occasionally, also, eleven-vertex [*nido*-7-$SB_{10}H_{12}$] (compound **5**, schematic cluster geometry **V**) is also observed, identifiable by NMR spectroscopy [34,35]. These yields appear to be very critically dependent upon the purity, age and history of the starting $[SB_8H_{12}]$ substrate; here it is recognized that sealed samples of $[SB_8H_{12}]$ under inert atmosphere or vacuum soon become yellow and develop a gelatinous appearance [36], although the natures of the products under these last conditions have not been described.

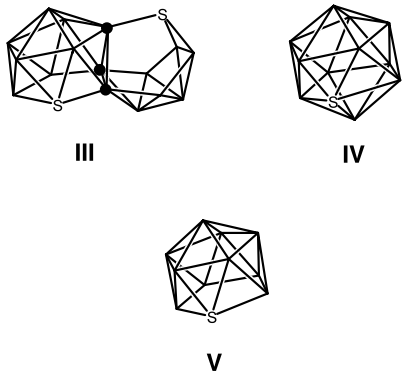


The known 12-vertex [*closo*-$SB_{11}H_{11}$] species **4** is readily separated from **2** and **3** by chromatography on silica, and identified by NMR spectroscopy [32]. Of the two $[S_2B_{16}H_{16}]$ isomers, the pure *n*-isomer **2** can most readily be obtained by column chromatography and recrystallisation. By contrast, the *iso* species **3** has required more meticulous thin-layer chromatographic work, followed by final HPLC purification, to generate clean samples free from compounds **2** and **4**, and, when present, compound **5** also. Purification of compound **2** is easier because it is the first eluted component of a complex chromatographic band, and therefore an initial cut can generate a pure sample, whereas compound **3** overlaps with the 'tail' of the chromatographic band of compound **2**. Purification of **3** is additionally hampered in that it is less robust in solution, and decomposes to generate [*nido*-7-$SB_{10}H_{12}$] (**5**) and an unidentified intractable residue. Here it may be noted that, as with the two $[B_{18}H_{22}]$ isomers [18], the macropolyhedral [*n*-$S_2B_{16}H_{16}$] species **2** is relatively acidic. Reaction of a

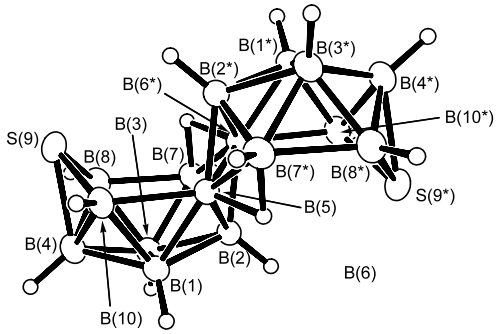


Fig. 1. Crystallographically determined molecular structure of the *n*-isomer of $[S_2B_{16}H_{16}]$ (**2**). There is crystallographic twofold symmetry. Selected interatomic distances (Å) are: S(9) to B(4) 1.963(2), B(8) 1.864(2), B(10) 1.846(2); B(7)–B(8) 1.909(2), B(5)–B(10) 1.905(2), B(6*)–B(7) 1.803(2), B(2)–B(6*) 1.757(2), B(5)–B(6*) 1.752(3). The angle B(8)–S(9)–B(10) is 100.07(7)°.

diethylether solution with NaH and precipitation of the resulting bright yellow $[n\text{-}S_2B_{16}H_{15}]^-$ anion **6** with $[PPh_4]Cl$ yields $[PPh_4][S_2B_{16}H_{15}]$ (compound **6a**, 78%). The $[tmndH]^+$ salt **6b** of anion **6** may be obtained more directly by the reaction of tmnd with neutral **2** in dichloromethane; here tmnd is an abbreviation for the non-nucleophilic proton acceptor *N*,*N*,*N*′,*N*′-tetramethylnaphthalene-1,8-diamine.

The two $[S_2B_{16}H_{16}]$ species **2** and **3** obviously derive from the oxidative combination of two $[SB_8H_{12}]$ residues (Eq. (1)), but the origin of the twelve-vertex *closo* species $[SB_{11}H_{11}]$ (**4**) is less rationalisable. However, it is noted that *closo* twelve-vertex $[B_{12}H_{12}]^{2-}$ has been observed as a reaction product when eighteen-vertex [*anti*-$B_{18}H_{22}$] is treated with base [37] and, because the $[n\text{-}S_2B_{16}H_{16}]$ isomer **2** from this present system has the architecture of [*anti*-$B_{18}H_{22}$], there may be parallels.

$$2SB_8H_{12}(\mathbf{1}) \rightarrow S_2B_{16}H_{16}(\mathbf{2} \text{ and } \mathbf{3}) + 4H_2 \qquad (1)$$

Both $[S_2B_{16}H_{16}]$ isomers **2** and **3** are reasonably air-stable, and can be handled in air for extended periods without apparent change, especially in the pure crystalline state. Fig. 1 is a representation of the crystallographically determined molecular structure of the *n*-$S_2B_{16}H_{16}$ isomer (compound **2**, schematic structure **II B**). Its general architecture (schematic cluster geometry **II** above) resembles that of [*anti*-$B_{18}H_{22}$] (compound **7**, schematic geometry **VI** below) in detail of its interatomic dimensions. Additionally, its $^{11}$B-NMR chemical-shift pattern exhibits parallels with both [*anti*-$B_{18}H_{22}$] (**7**) and with [*nido*-6-$SB_9H_{11}$] (**8**). The NMR behaviour has been discussed in sufficient detail previously [21]. For convenient reference, however, the $^{11}$B- and $^1$H-NMR chemical shifts of compound **2** are summarized in Table 1. The structural analogies among compound **2**, [*anti*-$B_{18}H_{22}$] (**7**) and [*nido*-6-$SB_9H_{11}$] (**8**) thus permit a description of the overall architecture of **2** in terms of a shared-edge, symmetrical fusion of two *nido* ten-vertex {$SB_9$} sub-clusters with two boron atoms in common as shown in the schematic representation **II C**. Structurally, there are few exceptional features, if any, in the interatomic dimensions of **2**. In line with the *nido*-decaboranyl subcluster descriptor, there are characteristically long *nido*-decaboranyl 'gunwale' distances, for example, the B(5)–B(10) distance is 1.905(2) Å. This, however, is some 0.07 Å shorter than the otherwise equivalent distance of 1.976(4) Å in [*anti*-$B_{18}H_{22}$] (**7**) [38].

Table 1
Measured NMR chemical shifts (in ppm) for $[n\text{-}S_2B_{16}H_{16}]$ (**2**) and for the $[n\text{-}S_2B_{16}H_{15}]^-$ anion **6** in $[PPh_4][n\text{-}S_2B_{16}H_{15}]$ (**6a**) in $CDCl_3$ solution at 293 K

| Assignment [a] | $\delta(^{11}B)$ (**2**) [b] | $\delta(^1H)$ (**2**) [b] | $\delta(^{11}B)$ (**6**) | $\delta(^1H)$ (**6**) |
|---|---|---|---|---|
| 1 | −0.6 | +3.06 | −7.2 | +2.58 |
| 2 | −17.9 | +0.96 | −15.3 | +0.43 |
| 3 | +8.1 | +3.61 | +8.2 | +3.30 |
| 4 | −30.4 | +0.71 | −29.4 | +0.59 |
| 5,6′ | +5.0 | [*conjuncto* site] | +21.4 | [*conjuncto* site] |
| 6,7′ | +5.0 | [*conjuncto* site] | +1.1 | [*conjuncto* site] |
| 7 | −20.7 | +2.33 | −25.9 | +1.69 |
| 8 | +16.6 | +4.75 | +7.3 | +3.91 |
| 10 | +27.3 | +5.38 | +28.0 | +5.04 |
| 1′ | +8.1 | +3.61 | +8.2 | +3.30 |
| 2′ | −17.9 | +0.96 | −8.0 | +0.77 |
| 3′ | −0.6 | +3.06 | −2.7 | +2.41 |
| 4′ | −30.4 | +0.71 | −30.6 | +0.84 |
| 5′ | −20.7 | +2.33 | −0.4 | +2.78 |
| 8′ | +27.3 | +5.38 | +19.3 | +4.40 |
| 10′ | +16.6 | +4.75 | −2.7 | +2.70 |
| μH | – | −1.99 | – | −3.00 |

[a] Assignments from [$^{11}$B–$^{11}$B]-COSY, $^1$H-{$^{11}$B(selective)} and [$^1$H–$^1$H]-COSY-{$^{11}$B(broadband)} experiments.
[b] Data from Ref. [26]. For convenience of comparison, there is duplication of entries for this symmetrical species.

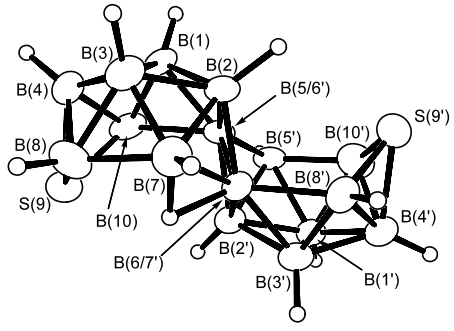


Fig. 2. Crystallographically determined molecular structure of the $[n\text{-}S_2B_{16}H_{15}]^-$ anion **6** in the $[tmndH][n\text{-}S_2B_{16}H_{15}]$ salt (**6b**). Selected interatomic distances (Å) are: S(9) to B(4) 1.928(8), B(8) 1.856(10), B(10) 1.882(9); S(9′) to B(4′) 1.966(8), B(8′) 1.811(9), B(10′) 1.892(11); B(2)–B(6,7′) 1.768(9), B(2′)–B(5,6′) 1.773(9), B(7)–B(8) 1.842(13), B(5/6′)–B(10) 1.937(11), B(6/7′)–B(8′) 1.894(10), B(5′)–B(10′) 1.809(13), B(6/7′)–B(7) 1.754(10), B(5/6′)–B(5′) 1.730(10), B(5/6′)–B(6/7′) 1.760(13), B(5/6)–B(10′) 1.937 (11). The angle B(8)–S(9)–B(10) is 99.0(3)° and the angle B(8′)–S(9′)–B(10′) is 98.0(3)°.

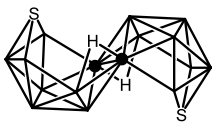


II B

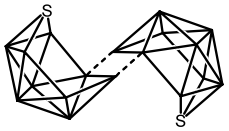


II C

A single-crystal X-ray diffraction study of the [*n*-$S_2B_{16}H_{15}]^-$ anion **6** in its $[tmndH]^+$ salt **6b** has also been carried out (Fig. 2 and schematic cluster structure **VII**). The structure of anion **6** is related to that of neutral **2** (schematic cluster structure **II B**) by a straightforward deprotonation at one of the bridging hydrogen sites. The slight contraction in the B(5)–B(10) intermolecular distance noted for the neutral [*n*-$S_2B_{16}H_{16}$] species **2**, when compared to that in [*anti*-$B_{18}H_{22}$] **7**, is also noted for its conjugate anion **6**. This latter behaviour may be compared to that of the anion in [tmndH][*anti*-$B_{18}H_{21}$] [39] compared to neutral [*anti*-$B_{18}H_{22}$]. Here, the asymmetry introduced by the deprotonation increases the contraction further for the equivalent positions in the [*anti*-$B_{18}H_{21}]^-$ anion. Thus, for example, B(7)–B(8) becomes 1.842(13) in [*anti*-$B_{18}H_{21}]^-$ versus 1.974(4) Å in [*anti*-$B_{18}H_{22}$].

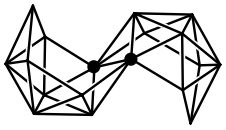

VI

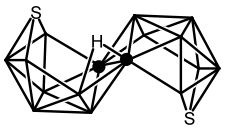


VII

The NMR properties of anion **6** (Table 1) readily relate to those of its neutral parent **2**. The $^{11}B$ and $^{1}H$ chemical shifts of the undeprotonated subcluster of **6** closely mimic those of the [*n*-$S_2B_{16}H_{16}$] parent **2**. The only marked exception to this generalisation is the *conjuncto* $^{11}B(5,6')$ position associated with the site of deprotonation. In the deprotonated subcluster (primed atoms in Fig. 2 and Table 1) there are big differences in $^{11}B$ shielding at the deprotonated $^{11}B(5,6')$ and $^{11}B(5')$ sites, and there are significant, but less marked, changes at sites adjacent to the deprotonated B(5′)–B(6′) link, but otherwise the *nido* ten-vertex shielding patterns of the undeprotonated subcluster and of neutral **2** [21] are essentially parallelled.

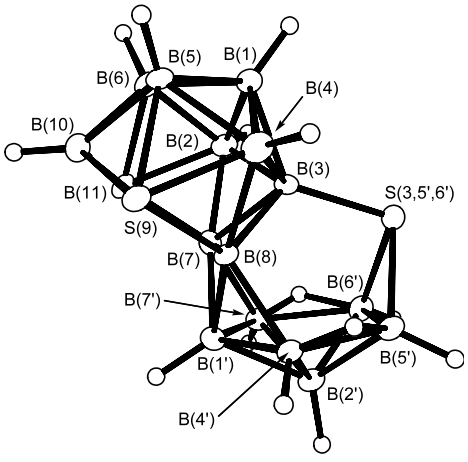


Fig. 3. Crystallographically determined molecular structure of the *iso*-isomer of [$S_2B_{16}H_{16}$] (**3**). There is also an *exo*-terminal hydrogen atom on B(11) and a bridging hydrogen atom spanning B(10)–B(11). They were not located in the X-ray diffraction analysis due to an unresolved positional disorder between the B(11) and S(9) positions across the pseudo mirror plane defined by B(1)B(1)B(3)S(3,5′,6′)B(6′)B(2′)B(1′), but they are apparent from NMR spectroscopy (Table 2 and text). Selected interatomic distances (Å) are: S(3,5′,6′) to B(3) 1.892(4), B(5′) 1.972(4), B(6′) 1.952(4); S(9)–B(8) 1.907(4), S(9)–B(10) 1.971(4), B(10)–B(11) 1.946(5), B(7)–B(8) 1.753(5), B(4′)–B(5′) 1.825(6), B(5′)–B(6′) 1.921(6), B(6′)–B(7′) 1.838(6). Angles at S(3,5′,6′) are: B(3)–B(5′) 96.6(2), B(3)–B(6′) 96.5(2), B(5′)–B(6′) 58.7(2)°.

The [*iso*-$S_2B_{16}H_{16}$] species **3** (Fig. 3, schematic cluster structure **III A** below) has also been structurally characterised by a single-crystal X-ray diffractions analysis, and is shown to be of a more unusual constitution that has several interesting structural parallels. The simplest structural analysis involves it being regarded as based on the conjunction of a *nido* 11-vertex {$SB_{10}$} subcluster and a *nido* eight-vertex {$B_8$} subcluster with a common, shared, two-boron edge (schematic geometry **III B**). In addition, the two subclusters are linked by a divalent sulphur bridge that takes the place (a) of a bridging hydrogen atom that would be in the B(5′,6′) position in a non-thiolated eight-vertex *nido* {$B_8$} unit and, similarly, (b) of an *exo*-terminal hydrogen atom at B(3) on the 11-vertex *nido* {$SB_{10}$} subcluster. Overall the molecular configuration resembles that of [$B_{16}H_{20}$] [40], in which each of the sulphur atoms replaces two hydrogen atoms (schematic geometry **III C**). The shared two-boron edge is a common feature in fused clusters and may be found in, for example, the binary boranes [$B_{12}H_{16}$] [41], [$B_{16}H_{20}$] [40], the *syn* and *anti* [$B_{18}H_{22}$] isomers [38], several macropolyhedral thiaboranes [42–45] and, of course, the structural isomer of **3**, compound **2**. Compounds possessing both a two-boron shared edge and a bridging atom acting as an *exo*-terminal moiety on the opposite subcluster are [$(CO)(PMe_3)_2IrB_{16}H_{14}Ir(CO)(PMe_3)_2$] [21], in [$(PMe_2Ph)_2PtB_{26}H_{26}(PMe_2Ph)$] [46] and in [$(PMe_2Ph)_2Pt$-$\eta^1,\eta^2$-*anti*-$B_{18}H_{20}$] [47].

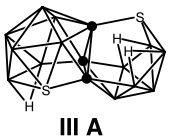


III A

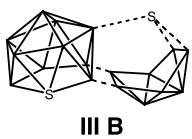


III B

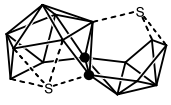


III C

One of a number of alternative interesting perspectives is to regard the architecture of compound **3** as a conjunction between a conventional 11-vertex *nido*

Table 2
Measured NMR chemical shifts (in ppm) for [*iso*-$S_2B_{16}H_{16}$] (**3**) together with $\delta(^{11}B)$ values for corresponding positions in [$SB_{10}H_{12}$] (**5**) [a] [$B_8H_{12}$] (**9**) [b] and [$S_2B_{16}H_{14}(PPh_3)$] (**10**) [c] for comparison

| Assignment [d] | $\delta(^{11}B)$ (**3**) [d] | $\delta(^{1}H)$ (**3**) [d] | $\delta(^{11}B)$ (**5**)/(**9**) | $\delta(^{11}B)$ (**10**) |
|---|---|---|---|---|
| 1 | −23.7 | +2.08 | −17.7 | −24.9 |
| 2 | −24.4 | +1.68 | −25.1 | −27.0 |
| 3 | −3.4 | [S bridge] | −25.1 | −9.6 |
| 4 | +12.2 | +3.77 | +16.4 | +14.7 |
| 5 | −3.9 | +3.17 | −1.7 | −4.5 |
| 6 | −5.8 | +2.87 | −1.7 | −5.3 |
| 7/8′ [e] | +18.7 | [*conjuncto* site] | −10.8/+7.5 | +19.1 |
| 8/3′ [e] | +2.1 | [*conjuncto* site] | −4.0/+7.5 | +1.4 |
| 9 | [S] | [S] | [S] | [S] |
| 10 | −2.9 | +3.00 [f] | −4.0 | −3.0 |
| 11 | −19.9 | +1.57 [f] | −10.8 | −20.0 |
| 1′ | +15.7 | +4.56 | −2.0 | −6.7 |
| 2′ | −41.5 | +0.59 | −22.0 | −42.2 |
| 3′/8 [e] | +2.1 | [*conjuncto* site] | +7.5/−4.0 | +1.4 |
| 4′ | −31.4 | +1.46 [g] | −19.4 | −30.9 |
| 5′ | −6.0 | +2.87 [g] | +7.5 | −6.7 |
| 6′ | −2.6 | +3.10 [h] | +7.5 | +0.6 |
| 7′ | −30.5 | +1.63 [h] | −19.4 | −29.9 |
| 8′/7 [e] | +18.7 | [*conjuncto* site] | +7.5/−10.8 | +19.1 |

[a] Data from Ref. [48].
[b] Data from Ref. [49].
[c] Data from Ref. [50].
[d] Assignments from [$^{11}B$–$^{11}B$]-COSY, $^{1}H$-{$^{11}B$(selective)} and [$^{1}H$–$^{1}H$]-COSY-{$^{11}B$(broadband)} experiments.
[e] Table entries for these positions repeated for convenience of comparison.
[f] Additionally μH(10,11) at −1.95 ppm.
[g] Additionally μH(4,5′) at −1.22 ppm.
[h] Additionally μH(6′,7′) at −0.98 ppm.

$\{SB_{10}\}$ unit, as above, and a 'remote-*arachno*' ten-vertex $\{SB_9\}$ unit, as in schematic geometry **VIII** below. The remote-*arachno* $\{SB_9\}$ geometry **IX** is derived by the removal of two non-adjacent, mutually *meta*, vertices from the *closo* 12-vertex icosahedron (schematic **X**). The recognition of this new subcluster type engenders speculation on the possible future isolation of stable single-cluster examples of this remote-*arachno* ten-vertex geometry **IX**.

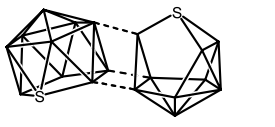

VIII


IX


X

Measured NMR data for the new [*iso*-$S_2B_{16}H_{16}$] species **3** are in Table 2, together with $^{11}B$ values for the related single-cluster comparators [*nido*-7-$SB_{10}H_{12}$] (**5**) [48] and [*nido*-$B_8H_{12}$] (**9**) [49]. The phosphine-substituted species [*iso*-$S_2B_{16}H_{14}$-1′-($PPh_3$)] (compound **10**; schematic structure **XII**) is also included for comparison. This analogue of compound **3**, together with the structurally related nickel species [$(PPh_3)NiS_2B_{16}H_{12}(PPh_3)$] (compound **11**, schematic cluster geometry **XIII**), have been previously described and characterised [50]. They were isolated in low yield from the reaction of [$NiCl_2(PPh_3)_2$] with [*n*-$S_2B_{16}H_{16}$] (**2**). For the *iso* compound **3**, sufficient NMR cross-correlations were obtained from [$^{11}B$–$^{11}B$]-COSY experiments, and these, together with $^{1}H$-{$^{11}B$(selective)} and [$^{1}H$–$^{1}H$]-COSY-{$^{11}B$(broadband)} experiments, enabled most of the $^{11}B$ and $^{1}H$ assignments to be made.

The structural similarities of the two subclusters of compound **3** to those of [*nido*-7-$SB_{10}H_{12}$] (**5**) and [*nido*-$B_8H_{12}$] (**8**) invite a spectroscopic comparison. The $^{11}B$ NMR chemical shifts for the eleven-vertex $\{SB_{10}\}$ subcluster in compound **3** are broadly similar to those in [*nido*-7-$SB_{10}H_{12}$] (**5**) for boron nuclei remote from the positions of conjunction, though shifted generally slightly to higher field, by +1 to −9 ppm. Conversely, the positions of conjunction—B(3), B(7), B(8)—are shifted downfield by +22, +28 and +6 ppm, respectively. The *nido* $\{B_8\}$ subcluster shows considerably more variation compared to single-cluster [*nido*-$B_8H_{12}$] (**8**). This bigger variation is to be expected since all vertices in the $\{B_8\}$ unit are either *conjuncto* linkage sites, sulphur-bridged or adjacent to these positions. The general trend is again to higher field, although the basic [*nido*-$B_8H_{12}$] shielding pattern is still traceable. The proton spectrum of compound **3** is of particular importance because it shows the presence of an *exo*-terminal hydrogen atom on the B(11) position of the *nido* $\{SB_{10}\}$ subcluster, and three bridging hydrogen atoms, at the (10,11), (4′,5′) and (6′,7′) positions. Only two of these four, at the (4′,5′) and (6′,7′) bridging positions on the *nido* $\{B_8\}$ subcluster, were located in the X-ray diffraction analysis. The bridging hydrogen atom spanning B(10)–B(11), and an associated *exo*-terminal hydrogen atom on the B(11) vertex of the $\{SB_{10}\}$ subcluster were not detectable from the diffraction data because of B(11)–S(9) disorder across the pseudo mirror plane defined by B(1)B(1)B(3)S(3,5′,6′)B(6′)B(2′)B(1′). Such positional disorder is not uncommon among S–$BH_2$ and $CH_2$–$BH_2$ positions in solid-state structural analyses.

The phosphine species [$S_2B_{16}H_{14}(PPh_3)$] (**10**) [50] warrants brief further mention. Its schematic structure **XII** compared to that of neutral [*iso*-$S_2B_{16}H_{16}$] (compound **3**, schematic molecular structure **XI**), demonstrates that the two-electron $PPh_3$ ligand replaces the one-electron hydrogen atom at the B(1′) position on the

$\{B_8\}$ subcluster, and that this subcluster correspondingly lacks the bridging hydrogen atom at the B(6′)B(7′) position, so that electron parity is maintained. Compounds **3** and **10** are thereby closely related. The report on $[S_2B_{16}H_{14}(PPh_3)]$ (**10**) did not assign the $^{11}B$ spectrum [50]. Assignments for compound **10** can now be made by comparison of its shielding behaviour relative to that of compound **3** (Table 2). However, these assignments are necessarily tentative in the absence of correlation experiments for compound **10**. The $\{SB_{10}\}$ subcluster of compound **10** will be relatively unperturbed compared to that of compound **3**, and so the assignments for this unit will be more reliable than those for the much more modified $\{B_8\}$ unit. Nevertheless, it is apparent that the general NMR shielding behaviour of compounds **3** and **10** is generally comparable.

As mentioned above, compound **10**, along with the structurally related nickel species $[(PPh_3)NiS_2B_{16}H_{12}(PPh_3)]$ (compound **11**, schematic cluster geometry **XIII**) were both isolated in low yield from the reaction of $[NiCl_2(PPh_3)_2]$ with the $[n\text{-}S_2B_{16}H_{16}]$ isomer **2**. The characterization now of the $[iso\text{-}S_2B_{16}H_{16}]$ isomer **3** (schematic structure **XI**), and the structural similarities apparent from a comparison of structures **XI** and **XIII**, now suggest that both species **10** and **11** could perhaps arise from impurities of the $[iso\text{-}S_2B_{16}H_{16}]$ isomer **3** in the samples of *n*-isomer **2** used, rather than via a rearrangement of the skeleton of the *n*-isomer **2** as at first thought [50]. We have observed no definitive interconversion of isomer **2** to isomer **3**, although it does appear that isomer **3** is less robust in solution. Both isomers are reasonably air-stable, and can be handled in air for extended periods without apparent change, especially in the pure crystalline state.

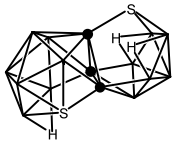


**XI**

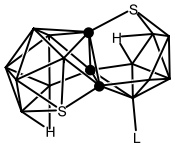


**XII**

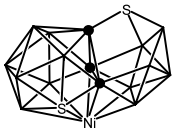


**XIII**

In the generation of the $[n\text{-}S_2B_{16}H_{16}]$ isomer **2**, the classical $[anti\text{-}B_{18}H_{22}]$ type of cluster geometry **VII** is generated. Geometrically, this is simply achieved by the connection of the two nine-vertex *arachno* cluster shapes of the $[SB_8H_{12}]$ starting compound **1** as in schematic **XIV**. This connection of geometries may therefore mimic the gross overall mechanism of fusion, although the overall reaction stoichiometry (Eq. (1) above) implies at least four sub-steps concomitant with the successive loss of four dihydrogen units.

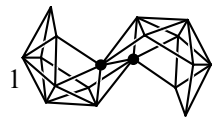


**VI**

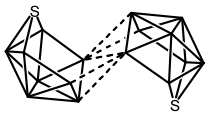


**XIV**

A similarly simple gross fusion picture for the formation of the $[iso\text{-}S_2B_{16}H_{16}]$ species **3** is not so straightforward. Its configuration **III** bears some superficial resemblance to the *syn* and the *anti* $B_{18}H_{22}$ types of configurations such as those drawn for $\{S_2B_{16}\}$ units in schematic geometries **XV** and **XVI**, respectively, but either of these, once formed, would require substantial rearrangement to generate the observed cluster geometry **III D** of compound **3**. Of these, an overall $[syn\text{-}B_{18}H_{22}]$ configuration cannot in any event be generated by the simple direct connection of two type-**I** *arachno* nine-vertex shapes. This last supposition tends to be confirmed experimentally: for example, it is found that thermolyses of $[B_9H_{13}(OBu_2)]$ or $[B_9H_{13}(SMe_2)]$ yield only the *anti* isomer of $[B_{18}H_{22}]$, with no *syn* isomer observed as a product [18,19].

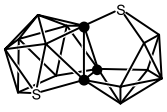


**III D**

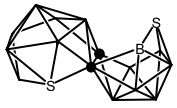


**XV**


**XVI**

The configuration of the $[iso\text{-}S_2B_{16}H_{16}]$ species **3** (schematic **III**) can, however, readily be visualised by a connection of the two *arachno* nine-vertex type-**I** $\{SB_8\}$ skeletons as in schematic **XVII**, with thence a relatively minor vertex movement of one sulphur atom one step along the open face of one of the incipient subclusters, but with all the other cluster atoms remaining in their starting positions, as in schematic **XVIII**. Overall, the formation of the *n*-isomer **2** can therefore be visualised as arising from the coming together of two open-face $\{B_3\}$ strings on the two starting *arachno* $\{SB_8\}$ geometries (schematic **XIV** above); and the *iso* species **3** by the coming together of two open-face $\{SB_2\}$ strings (schematics **XVII** and **XVIII** below).

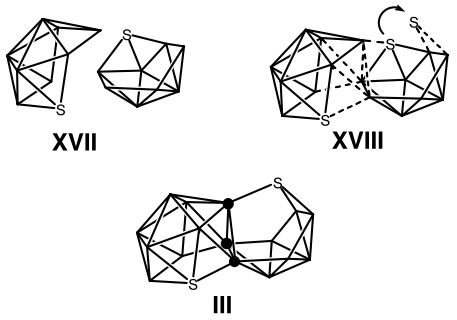


The terminology of cluster fusion processes is not yet developed, but the *n*-isomer **2** can be regarded as derived from what may be described as a symmetrical $<1{:}1>$ fusion mechanism, in that each cluster adds one vertex to the other cluster, so that two nine-vertex species generate a macropolyhedral assembly that consists of two ten-vertex subclusters. The *iso* species **3** would then derive from a $<2{:}0>$ fusion because one starting cluster adds two vertices to the other cluster but gains zero vertices in return, so that two nine-vertex clusters give a macropolyhedral assembly with one eleven-vertex subcluster and one nine-vertex subcluster.

These are of course gross architectural considerations. Mechanistically, as mentioned above, the elimination of four dihydrogen molecules (Eq. (1) above) implies a multistep process of at least four intermediate stages. Sufficient structural precedent is now emerging for a reasonable speculation about some of these intermediate mechanistic steps to be made. An understanding of the mechanisms of such processes of fusion will ultimately help to establish general transferable generic routes for intercluster fusion. At present, the lack of such generic fusion routes is inhibitory to a rapid development of the macropolyhedral area of boron-containing cluster chemistry.

Thus, in terms of general cluster geometrical patterns, initial steps in the formation of the [*n*-$S_2B_{16}H_{16}$] species **2** could involve a $<1{:}0>$ fusion of two [$SB_8H_{12}$] species **1**, as in schematic **XIX**, to form a *spiro*-type intermediate **XX**, possibly of formulation {$S_2B_{16}H_{20}$}. Precedents for this type of linkage are found in [$S_2B_{18}H_{20}$] [51] and [$(PMe_2Ph)_2Pd_2B_{16}H_{22}(PMe_2Ph)_2$] [24]. A subsequent condensation step could then involve the generation of an additional interboron linkage such as in structure **XXI**. Precedents for this type of linkage are observed in the $[S_2B_{17}H_{18}]^-$ and $[S_2B_{18}H_{19}]^-$ anionic systems [29,42,51] and in neutral [$(PMe_2Ph)_3Pt_2B_{16}H_{20}$($PMe_2Ph$)] [24]. Of the compounds just mentioned, the palladium and platinum species are believed to represent successive initial intermediates in the formation of more intimately condensed macropolyhedrals from the *arachno* nine-vertex species [$(PMe_2Ph)_2PdB_8H_{12}$] and [$(PMe_2Ph)_2PtB_8H_{12}$], respectively [17,24], which may indicate that two steps of this nature may be common features of initial autofusion steps of *arachno* nine-vertex species. A further condensation along the sequence **XX** → **XXI** → **II** would then occur to give the observed [*n*-$S_2B_{16}H_{16}$] configuration **II** of compound **2**.

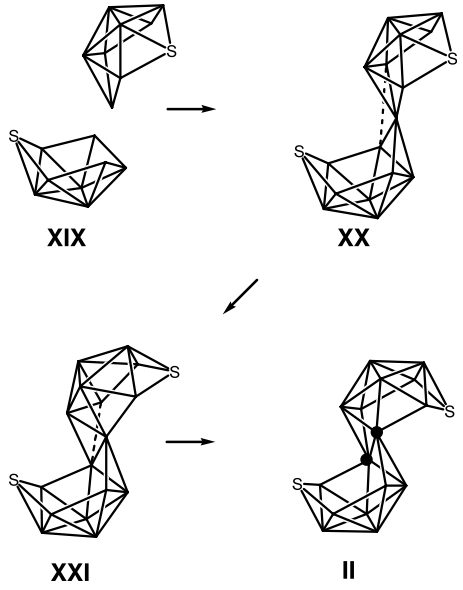


For the generation of the [*iso*-$S_2B_{16}H_{16}$] isomer **3**, a related mutual approach and subsequent $<1{:}0>$ condensation of two [$SB_8H_{12}$] species **1** can be postulated (schematics **XXII** and **XXIII**), but now with an alternative mutual positioning of the merging faces to give an alternative *spiro* intermediate **XXIII**. This intermediate **XXIII** would then be a precursor to the [*iso*-$S_2B_{16}H_{16}$] isomer **3** (schematic **XXX**) via an alternative type of closure involving the hop of the incipient bridging sulphur atom one position around the open face of the incipient *nido* {$B_8$} subcluster as represented in **XXIX**.

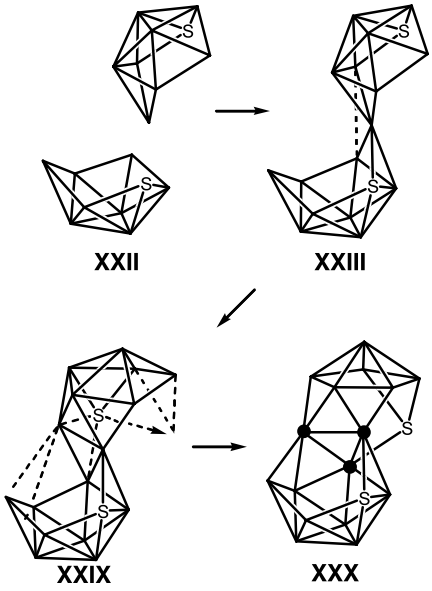

## 3. Conclusions

The thermolysis of the *arachno* nine-vertex thiaborane $[SB_8H_{12}]$ (**1**) generates the $[n\text{-}S_2B_{16}H_{16}]$ isomer that has an $[anti\text{-}B_{18}H_{22}]$ type of configuration. The formation of this product is in analogy with the thermolyses of *arachno* nine-vertex $[B_9H_{13}(SMe_2)]$ and $[B_9H_{13}(O^nBu_2)]$ that generate $[anti\text{-}B_{18}H_{22}]$ itself [18,19]. However, the formation of the $[iso\text{-}S_2B_{16}H_{16}]$ isomer **3** of quite different configuration has no precedent in the $[B_9H_{13}L]$ reactions, and augurs well for the continued generation of interesting new macropolyhedral architectures from the thermolyses, or other oxidative condensations, of other nine-vertex main-group *arachno* heteroboranes such as $[HNB_8H_{12}]$ and $[H_2CB_8H_{12}]$, although such products may occur only in low yield and therefore be difficult to separate and purify. These considerations are reinforced by the observation that the thermolysis of the closely related *arachno* nine-vertex thiaborane $[SB_8H_{10}(SMe_2)]$ generates, in $[S_2B_{17}H_{17}(SMe_2)]$, yet another interesting new macropolyhedral structural type [20], suggesting that a general examination of condensation reactions of other thiaboranes $[SB_8H_{10}L]$ [52,53], as well as corresponding azaboranes and carbaboranes $[HNB_8H_{12}]$, $[HNB_8H_{10}L]$, $[H_2CB_8H_{12}]$, $[RHCB_8H_{12}]$ and $[H_2CB_8H_{10}L]$ [53–57], should reveal even further additional examples of interesting unanticipated macropolyhedral architectures.

## 4. Experimental

### 4.1. General

Reactions were carried out in dry solvents (diethylether, hexane, cyclohexane and dichloromethane) under dry nitrogen, but subsequent manipulatory and separatory procedures were carried out in air. Preparative thin-layer chromatography (TLC) was carried out using 1 mm layers of silica gel G (Fluka, type GF254) made from water slurries on glass plates of dimensions 20 cm × 20 cm, followed by drying in air at 80 °C; components were located visually under ultra-violet irradiation. Column chromatography was monitored by analytical TLC using silica gel G on aluminium foil (Siluflol (Kavalier, Prague)) as stationary phase, with components being detected by iodine vapour, followed by aqueous $AgNO_3$ spray; analytical $R_F$ values are given for this stationary phase. HPLC was performed on a Lichosorb SI 60 column, dimensions 25 cm × 2.12 cm. Mass spectrometry was carried out on a VG Autospec instrument using electron-impact ionisation at 70 eV. NMR spectroscopy was performed at ca. 5.9, 9.4 and 11.8 T (fields corresponding to 250 and 400 and 500 MHz $^1H$ frequencies, respectively) using commercially available instrumentation and using techniques and procedures as adequately described and enunciated elsewhere [58–64]. Chemical shifts $\delta$ are given in ppm relative to $\Xi = 100$ MHz for $\delta(^1H)$ ($\pm 0.05$ ppm) (nominally TMS) and $\Xi = 32.083972$ MHz for $\delta(^{11}B)$ ($\pm 0.5$ ppm) (nominally $Et_2OBF_3$ in $CDCl_3$) [58]. $\Xi$ is as defined by McFarlane [65].

### 4.2. Isolation of compounds from the thermolysis of [arachno-4-$SB_8H_{12}$] (1)

A typical procedure was as follows. A sample of $[SB_8H_{12}]$ (**1**; 790 mg; 6.1 mmol) was prepared from $Cs^+[SB_9H_{12}]^-$ (2.76 g; 100 mmol) by literature procedures [33] and dissolved in anhydrous cyclohexane (30 ml). The solution was stirred and slowly heated to reflux temperature under an atmosphere of dinitrogen. The initially colourless solution slowly became yellow, then orange, and a deep yellow–orange solid precipitated. This solid product of low solubility is not yet investigated in detail, and is currently believed to consist of {SBH} polymers. After 1 h no further reaction was apparent, and monitoring by NMR spectroscopy showed that all the starting compound **1** was consumed. The solvent was evaporated in vacuo (room temperature and water pump), and the resinous residue extracted with dichloromethane (2 × 20 ml) and filtered. Monitoring by integrated $^{11}B$-NMR spectroscopy at this stage indicated the presence of four compounds in solution, subsequently shown to be **2**, **3**, **4** and **5**, in the approximate relative molar proportions 20:20:4:1, respectively. The filtrate was subjected to column chromatography (2 cm × 25 cm, silica gel, 70–220 mesh) using a mixture of hexane–dichloromethane (1:1) as mobile phase. The first pale yellow fraction **A**, $R_F$ ca. 0.7 ($CH_2Cl_2$), was $[closo\text{-}SB_{11}H_{11}]$ (**4**) (9 mg, 56 μmol, 0.9%). One principal yellow fraction **B** was apparent, $R_F$ 0.2–0.4 ($CH_2Cl_2$), which was separated, thence to yield a semi-crystalline solid upon evaporation. Change of solvent to a 50:50 MeCN–$CH_2Cl_2$ mixture gave a further yellow fraction **C**, $R_F$ ca. 0.8 (50:50 $CH_2Cl_2$:MeCN), characterized as $[nido\text{-}7\text{-}SB_{10}H_{12}]$ (**5**) (3 mg, 20 μmol, 0.3%). Component **B** was subjected to repeated preparative TLC using benzene and hexane–dichloromethane mixtures as mobile phases. This procedure yielded a substantial broad orange–yellow band on the chromatographic plates, $R_F$ ca. 0.7 (60:40 $C_6H_{14}$:$CH_2Cl_2$), which was identified by integrated $^{11}B$-NMR spectroscopy as an approximately equimolar mixture of $[n\text{-}S_2B_{16}H_{16}]$ (**2**) and $[iso\text{-}S_2B_{16}H_{16}]$ (**3**). The cutting of an initial fraction from this band directly can generate small pure samples of compound **2**. At this stage, further purification of the solid mixture that consists of both of the $[S_2B_{16}H_{16}]$ isomers **2** and **3** could be effected by sublimation at 90 °C/1.3 Pa. Pure individual compounds were thence obtained by pre-

parative HPLC ($CH_2Cl_2$:hexane 35:65, flow rate 10 ml $min^{-1}$); [*n*-$S_2B_{16}H_{16}$] (**2**) $R_T$ 6.1 min; [*iso*-$S_2B_{16}H_{16}$] (**3**) $R_T$ 7.0 min. The above is a typical procedure: as mentioned in the text, good reproducibility has not been attained in this reaction and separation. Starting from 2.5–3.0 g of $Cs[SB_9H_{12}]$, isolated yields from these procedures have been in the ranges 4–18% for compound **2**, and 2–4% for compound **3**. Compound **4** was obtained typically at 5–13%. Monitoring of these processes by integrated $^{11}$B-NMR spectroscopy shows that, under extended manipulation in solution in air, compound **2** appears to degrade slowly to give compound **4**, and compound **3** more rapidly gives compound **5**. Pale yellow single crystals of compound **3** were obtained by slow sublimation (ca. 3 months) in vacuo in a sealed 5 mm o.d. glass NMR tube positioned on a warm surface ($\approx 40$ °C) so that there was a slight temperature gradient along the tube towards a room temperature of ca. 21 °C. Pale yellow single crystals of compound **2** were obtained by slow evaporation of solvent from a solution of compound **2** in $CDCl_3$.

### 4.3. Preparation of [$PPh_4$][$S_2B_{16}H_{15}$] (**6a**)

To a solution of [*n*-$S_2B_{16}H_{16}$] (**2**, 100 mg, 400 μmol) in diethylether (15 ml) was added excess NaH (60% suspension in mineral oil, corresponding to 50 mg, 1.25 mmol) and the mixture stirred under a dinitrogen atmosphere for 1 h. The solution was then filtered and the filtrate added to a solution of $[PPh_4]Cl$ (0.2 g, 0.56 mmol) in $CH_2Cl_2$ (30 ml). The precipitate was filtered off, the solvent removed from the filtrate (ambient temperature, water pump) and the resultant orange solid recrystallised from $CH_2Cl_2$/hexane giving bright yellow $[PPh_4][S_2B_{16}H_{15}]$ (**6a**, 0.31 mmol, 78%). Crystals of the $[tmndH]^+$ salt of the $[S_2B_{16}H_{15}]^-$ anion **6** suitable for a single-crystal X-ray diffraction study were obtained by hexane diffusion into a dichloromethane solution containing equivalent molar quantities of 1,8-bisdimethylaminonapthalene (tetramethylnaphthalenediamine, tmnd) and [*n*-$S_2B_{16}H_{16}$] (**2**) to yield [tmndH][*n*-$S_2B_{16}H_{15}$] (**6b**).

### 4.4. X-ray crystallography

Crystal data for [*n*-$S_2B_{16}H_{16}$] (**2**): $H_{16}B_{16}S_2$: $M = 253.21$, monoclinic (from $CDCl_3$), Space group $P2_1/n$, $a = 7.0973(4)$, $b = 10.3570(7$, $c = 9.8348(6)$ Å, $\beta = 108.821(5)°$, $U = 684.27(7)$ Å$^3$, $Z = 2$, Mo–$K_\alpha$, $\lambda = 0.71073$ Å, $\mu = 3.102$ mm$^{-1}$, $T = 293(2)$ K, $R_1 = 0.0367$ for 1132 reflections and $wR_2 = 0.1147$ for all 2264 unique reflections; CCDC deposition number 198885. Crystal data for [*iso*-$S_2B_{16}H_{16}$] (**3**): $H_{16}B_{16}S_2$: $M = 253.21$, monoclinic (from a vacuum sublimation), Space group $P2_1$, $a = 6.88580(10)$, $b = 8.7566(2)$, $c = 11.2096(6)$ Å, $\beta = 94.848(2)°$, $U = 673.48(4)$ Å$^3$, $Z = 2$, Mo–$K_\alpha$, $\lambda = 0.71073$ Å, $\mu = 0.350$ mm$^{-1}$, $T = 100(2)$ K, $R_1 = 0.0631$ for 2541 reflections and $wR_2 = 0.1749$ for all 10 921 unique reflections; CCDC deposition number 198883. Crystal data for [tmndH][$S_2B_{16}H_{15}$] (**6b**): $C_{14}H_{34}B_{16}N_2S_2$: $M = 467.51$, monoclinic (from hexane/dichloromethane), Space group $Cc$, $a = 12.6811(4)$, $b = 14.5844(5)$, $c = 15.1443(5)$ Å, $\beta = 108.420(3)°$, $U = 2658.1(2)$ Å$^3$, $Z = 4$, Cu–$K_\alpha$, $\lambda = 1.54184$ Å, $\mu = 1.841$ mm$^{-1}$, $T = 293(2)$ K, $R_1 = 0.0317$ for 2293 reflections and $wR_2 = 0.0918$ for all 2306 unique reflections; CCDC deposition number 198884. Methods and programs were standard [66]. Compound **3** exhibited a positional disorder, of a type not uncommonly found in polyhedral thiaborane compounds, for sulphur and boron atoms between the (9) and (11) positions on the 11-vertex $\{SB_{10}\}$ subcluster. This precluded the location of the associated *exo*-terminal hydrogen atom on B(11) and the bridging hydrogen atom spanning B(10)–B(11), but these were reasonably inferred from NMR spectroscopy (Table 2 and text).

## 5. Supplementary material

Crystallographic data for [*n*-$S_2B_{16}H_{16}$] (**2**), for [*iso*-$S_2B_{16}H_{16}$] (**3**) and for the $[tmndH]^+$ salt **6b** of the [*n*-$S_2B_{16}H_{15}]^-$ anion **6** are deposited at the Cambridge Crystallographic Data Centre, CCDC, deposition nos. 198885, 198883 and 198884, respectively. Copies of this information may be obtained free of charge from The Director, CCDC, 12 Union Road, Cambridge CB2 1EZ, UK (Fax: +44-1223-336033 e-mail: deposit@ccdc.cam.ac.uk or www: http://www.ccdc.cam.ac.uk).

## Acknowledgements

Contribution no. 87 from the Řež-Leeds Anglo-Czech Polyhedral Collaboration (ACPC). We thank the Grant Agency of the Academy of Sciences of the Czech Republic (grant no. A403 1402), the Ministry of Education of the Czech Republic (projects nos. LN00A028 and LB98233), The Royal Society (London), the UK EPSRC (grants nos. J/56929, K/05818, L/49505 and M/83360 and studentships to PKD and MGSL) for support, and the Royal Society of Chemistry for a Journals Grants for International Authors. Additional thanks are given to The British Council in Prague for support to MGSL.

## References

[1] (a) R.E. Williams, Inorg. Chem. 10 (1971) 210;
(b) R.E. Williams, Adv. Inorg. Chem. Radiochem. 18 (1986) 64.

[2] (a) K. Wade, Chem. Commun. (1971) 792;
(b) K. Wade, Adv. Inorg. Chem. Radiochem. 18 (1986) 1.
[3] D.M.P. Mingos, Nature (Phys. Sci.) 236 (1972) 99.
[4] G.B. Dunks, M.M. McKowan, M.F. Hawthorne, J. Am. Chem. Soc. 93 (1971) 2541.
[5] W.J. Evans, M.F. Hawthorne, J. Chem. Soc. Chem. Commun. (1974) 38.
[6] N.M.M. Wilson, D. Ellis, A.S.F. Boyd, B.T. Giles, S.A. Macgregor, G.M. Rosair, A.J. Welch, Chem. Commun. (2002) 464.
[7] A. Burke, D. Ellis, B.T. Giles, B.E. Hodson, S.A. Macgregor, G.M. Rosair, A.J. Welch, Angew. Chem. Int. Ed. 42 (2003) 225.
[8] R.N. Grimes, Angew. Chem. Int. Ed. 42 (2003) 1198.
[9] W. Jiang, D.E. Harwell, M.D. Mortimer, C.B. Knobler, M.F. Hawthorne, Inorg. Chem. 35 (1996) 4355.
[10] (a) J. Müller, K. Baše, T.F. Magnera, J. Michl, J. Am. Chem. Soc. 114 (1992) 9721;
(b) X. Yang, W. Jang, C.B. Knobler, M.F. Hawthorne, J. Am. Chem. Soc. 114 (1992) 9719.
[11] M.F. Hawthorne, in: W. Siebert (Ed.), Advances in boron chemistry, Royal Society of Chemistry, Cambridge, England, 1997, p. 261.
[12] M.R. Churchill, A.H. Reis, J.N. Francis, M.F. Hawthorne, J. Am. Chem. Soc. 92 (1970) 4993.
[13] X. Wang, M. Sabat, R.N. Grimes, J. Am. Chem. Soc. 117 (1995) 12227.
[14] H. Yao, M. Sabat, R.N. Grimes, F.F. de Biani, P. Zanello, Angew. Chem. Int. Ed. 42 (2003) 1002.
[15] J.D. Kennedy, in: W. Seibert (Ed.), Advances in boron chemistry, Royal Society of Chemistry, Cambridge, England, 1997, p. 451.
[16] J. Bould, W. Clegg, S.J. Teat, L. Barton, N.P. Rath, M. Thornton-Pett, J.D. Kennedy, in: Boron Chemistry at the Millennium, Special edition of Inorg. Chim. Acta 289 (1999) 95.
[17] (a) J. Bould, A. Franken, T. Jelínek, J.D. Kennedy, C.A. Kilner, M.G.S. Londesborough, M. Thornton-Pett, Abstracts Eleventh International Meeting on Boron Chemistry (IMEBORON XI), Moscow, Russia, July 28-August 2, 2002, Abstract no. IA-4, p. 29.;
(b) S.L. Shea, S.D. Perera, J. Bould, A. Franken, T. Jelínek, J.D. Kennedy, C.A. Kilner, M.G.S. Londesborough, M. Thornton-Pett, in: Y. Bubnov et al. (Eds.), Boron Chemistry at the Beginning of the 21st Century, Nauka, Moscow, in press.
[18] J. Plešek, S. Hermánek, B. Štíbr, F. Hanousek, Collect. Czech. Chem. Commun. 32 (1967) 1095.
[19] J. Dobson, P.C. Keller, R. Schaeffer, Inorg. Chem. 7 (1968) 399.
[20] P. Kaur, J. Holub, N.P. Rath, J. Bould, L. Barton, B. Štíbr, J.D. Kennedy, J. Chem. Soc. Chem. Commun. (1996) 273.
[21] L. Barton, J. Bould, J.D. Kennedy, N.P. Rath, J. Chem. Soc. Dalton Trans. (1996) 3145.
[22] M.A. Beckett, J.E. Crook, N.N. Greenwood, J.D. Kennedy, J. Chem. Soc. Dalton Trans. (1986) 1879.
[23] M.A. Beckett, N.N. Greenwood, J.D. Kennedy, P.A. Salter, M. Thornton-Pett, J. Chem. Soc. Chem. Commun. (1986) 556.
[24] M.G.S. Londesborough, E.J. MacLean, S.J. Teat, J. Bould, M. Thornton-Pett, J.D. Kennedy, in preparation for submission; see also M.G.S. Londesborough, E.J. MacLean, S.J. Teat, J. Bould, C.A. Kilner, M. Thornton-Pett, J.D. Kennedy, in: Y. Bubnov et al. (Eds.), Boron Chemistry at the Beginning of the 21st Century, Nauka Press, Moscow, in press.
[25] M.G.S. Londesborough, C.A. Kilner, M. Thornton-Pett, J.D. Kennedy, J. Organomet. Chem. 657 (2002) 262.
[26] T. Jelínek, J.D. Kennedy, B. Štíbr, J. Chem. Soc. Chem. Commun. (1994) 1415.
[27] J.D. Kennedy, Abstracts Ninth International Meeting on Boron Chemistry (IMEBORON IX), Heidelberg, Germany, July 14–18 1996, Abstract no. PL-5, p. 35.
[28] T. Jelínek, B. Štíbr, J.D. Kennedy, M. Thornton-Pett, Abstracts Ninth International Meeting on Boron Chemistry (IMEBORON IX), Heidelberg, Germany, July 14–18 1996, Abstract no. CA-4, p. 28.
[29] (a) J. Bould, D.L. Ormsby, H.-J. Yao, C.-H. Hu, J. Sun, R.-S. Jin, S.L. Shea, W. Clegg, N.P. Rath, M. Thornton-Pett, R. Greatrex, P.-J. Zheng, L. Barton, B. Štíbr, J.D. Kennedy. Abstracts Tenth International Meeting on Boron Chemistry (IMEBORON X), Durham, England, July 11–15 1999, Abstract no. CA-8, p. 7.;
(b) M.G. Davidson, A.K. Hughes, T.B. Marder, K. Wade (Eds.), Contemporary Boron Chemistry, Royal Society of Chemistry, Cambridge, England, 2000, p. 171.
[30] (a) T. Jelínek, J.D. Kennedy, S.A. Barrett, M. Thornton-Pett, I. Cisarová, Abstracts Tenth International Meeting on Boron Chemistry (IMEBORON X), Durham, England, July 11–16 1999, Abstract no. CB-19, p. 101.;
(b) V Ash, in: M.G. Davidson, A.K. Hughes, T.B. Marder, K. Wade (Eds.), Contemporary Boron Chemistry, Royal Society of Chemistry, Cambridge, England, 2000, p. 175.
[31] S.L. Shea, J. Bould, M.G.S. Londesborough, S.D. Perera, A. Franken, D.L. Ormsby, T. Jelínek, B. Štíbr, J. Holub, C.A. Kilner, M. Thornton-Pett, J.D. Kennedy, Pure Appl. Chem., in press.
[32] W.L. Smith, B.J. Meneghelli, D.A. Thompson, P.A. Klymco, N. McClure, R.W. Rudolph, Inorg. Chem. 16 (1977) 3008.
[33] J.H. Jones, K. Baše, B. Štíbr, J.D. Kennedy, X.L.R. Fontaine, N.N. Greenwoood, M.G.H. Wallbridge, Polyhedron 8 (1989) 2089.
[34] W.R. Hertler, F. Klanberg, E.L. Muetterties, Inorg. Chem. 6 (1967) 1696.
[35] J. Plešek, S. Hermánek, J. Chem. Soc. Chem. Commun. (1975) 127.
[36] K. Baše, V. Gregor, S. Hermánek, Chem. Ind. (London) (1979) 743.
[37] F.P. Olsen, R.C. Vasavanda, M.F. Hawthorne, J. Am. Chem. Soc. 90 (1967) 3946.
[38] P.G. Simpson, W.N. Lipscomb, J. Chem. Phys. 39 (1963) 26.
[39] J. Bould, T. Jelínek, J.D. Kennedy, M. Thornton-Pett, Acta Cryst. to be submitted for publication.
[40] L.B. Friedman, R.E. Cook, M.D. Glick, Inorg. Chem. 9 (1970) 1452.
[41] C. Brewer, R.G. Swisher, E. Sinn, R.N. Grimes, J. Am. Chem. Soc. 107 (1985) 3558.
[42] T. Jelínek, J.D. Kennedy, B. Štíbr, M. Thornton-Pett, Angew. Chem. Int. Ed. Engl. 33 (1994) 1599.
[43] T. Jelínek, J.D. Kennedy, B. Štíbr, M. Thornton-Pett, Inorg. Chem. Commun. 1 (1998) 179.
[44] T. Jelínek, I. Cisarová, B. Štíbr, J.D. Kennedy, M. Thornton-Pett, J. Chem. Soc. Dalton Trans. (1998) 2965–2967.
[45] T. Jelínek, C. Kilner, M. Thornton-Pett, J.D. Kennedy, J. Chem. Soc. Chem. Commun. (1999) 1905.
[46] J. Bould, W. Clegg, J.D. Kennedy, S.J. Teat, J. Chem. Soc. Dalton Trans. (1998) 2777.
[47] (a) Y.M. Cheek, N.N. Greenwood, J.D. Kennedy, W.S. McDonald, J. Chem. Soc. Chem. Commun. (1982) 80;
(b) Y.M. Cheek, unpublished observations, University of Leeds, Leeds, 1980-1984.
[48] W.F. Wright, A.R. Garber, L.J. Todd, J. Magn. Reson. 30 (1978) 595.
[49] R.R. Rietz, R. Schaeffer, L.G. Sneddon, Inorg. Chem. 11 (1972) 1242.
[50] P. Kaur, M. Thornton-Pett, W. Clegg, J.D. Kennedy, J. Chem. Soc. Dalton Trans. (1996) 4155.
[51] (a) D.L. Ormsby, T. Jelínek, S.L. Shea, R. Greatrex, B. Štíbr, J.D. Kennedy, in preparation.;
(b) See also Abstracts Tenth International Meeting on Boron Chemistry (IMEBORON X), Durham, England, July 11–15

1999, Abstract no. PA-38, p. 142;
(c) D.L. Ormsby, Computational Studies of Structure and Mechanism in Boron-containing Clusters, Thesis, University of Leeds, 2001.
[52] J. Holub, B. Štíbr, J.D. Kennedy, M. Thornton-Pett, T. Jelínek, Inorg. Chem. 33 (1994) 4545.
[53] J. Holub, J.D. Kennedy, B. Štíbr, Collect. Czech. Chem. Commun. 59 (1994) 367.
[54] T. Jelínek, B. Štíbr, J.D. Kennedy, Collect. Czech. Chem. Commun. 59 (1994) 2244.
[55] J. Plešek, B. Štíbr, X.L.R. Fontaine, T. Jelínek, M. Thornton-Pett, S. Hermánek, J.D. Kennedy, Inorg. Chem. 33 (1994) 2994.
[56] A. Franken, C.A. Kilner, M. Thornton-Pett, J.D. Kennedy, Collect. Czech. Chem. Commun. (J. Plešek Special Edition) 67 (2002) 869.
[57] A. Franken, C.A. Kilner, M. Thornton-Pett, J.D. Kennedy, J. Organomet. Chem. 657 (2002) 180.
[58] J.D. Kennedy, in: J. Mason (Ed.), Boron, Chapter 8 in Multinuclear NMR, Plenum, New York and London, 1987, p. 221 (and references therein).
[59] X.L.R. Fontaine, J.D. Kennedy, J. Chem. Soc. Chem. Commun. (1986) 779.
[60] J.D. Kennedy, J. Staves, Z. Naturforsch., Teil B 34 (1989) 808.
[61] X.L.R. Fontaine, J.D. Kennedy, J. Chem. Soc. Dalton Trans. (1987) 1573.
[62] M.A. Beckett, M. Bown, X.L.R. Fontaine, N.N. Greenwood, J.D. Kennedy, M. Thornton-Pett, J. Chem. Soc. Dalton Trans. (1988) 1969.
[63] G. Ferguson, J.D. Kennedy, X.L.R. Fontaine, Faridoon, T.R. Spalding, J. Chem. Soc. Dalton Trans. (1988) 2555.
[64] D. Reed, Chem. Soc. Rev. 22 (1993) 109.
[65] W. McFarlane, Proc. R. Soc. (London) Series A 306 (1968) 185.
[66] (a) Z. Otwinowski, W. Minor, DENZO-SMN, Processing of X-ray Diffraction Data Collected in Oscillation Mode, Methods Enzymol., C.W Carter, R.M. Sweet, (Eds.), Academic Press 276 (1997) 307.;
(b) COLLECT, Data Collection Strategy Program, Nonius, 1999.